Evaluation of Forest Decontamination Using Radiometric Measurements

Alan J. Cresswell[†*], *Hiroaki Kato*[‡], *Yuichi Onda*[‡], *Kenji Nanba*[†]

[†]Institute of Environmental Radioactivity, Fukushima University, 1 Kanayagawa, Fukushima 960-1296, Japan

[‡]Center for Research in Isotopes and Environmental Dynamics, University of Tsukuba, 1-1-1 Tennodai, Tsukuba, Ibaraki 305-8572, Japan

* Corresponding Author. Present address: Scottish Universities Environmental Research Centre, East Kilbride, Glasgow G75 0QF, UK. E-mail: alan.cresswell@glasgow.ac.uk

Abstract

An experiment has been conducted to evaluate the additional dose reduction by clear felling contaminated forestry in Fukushima Prefecture, Japan, and using the timber to cover the areas with wood chips. A portable gamma spectrometry system, comprising a backpack containing a 3x3" NaI(Tl) detector with digital spectrometer and GPS receiver, has been used to map dose rate and radionuclide activity concentrations before, after and at stages during this experiment. The data show the effect of the different stages of the experiment on dose rate at different locations around the site. The spectrometric data have allowed the assessment of the contributions of natural and anthropogenic radionuclides to the dose rate at different parts of the site before and after the experiment. This has clearly demonstrated the value of radiometric methods in evaluating remediation, and the effect of other environmental processes. The value of spectrometric methods which directly measure radionuclide concentrations has also been shown, especially through the identification of the contribution of natural and anthropogenic activity to the measured dose rate. The experiment has shown that clearing trees and applying wood chips can reduce dose rates by 10-15% beyond that achieved by just clearing the forest litter and natural redistribution of radiocaesium.

Keywords

Radiocaesium; Gamma Dose Rate; Fukushima Nuclear Accident

1. Introduction

Following the Fukushima Daiichi Nuclear Power Plant (FDNPP) accident in March 2011, large areas of Fukushima Prefecture were contaminated with radiocaesium. Approximately 70% of the contaminated area is forested, providing a reservoir for contamination that is largely recycled within the forests (Hashimoto et.al. 2013). Remediation of forests is particularly challenging, and current practice in Japan is to reduce the dose rate in and around buildings by the removal of forest litter and undergrowth to a distance of 20 m from roads and buildings. Decontamination model projects conducted by the Japan Atomic Energy Agency (JAEA) have demonstrated reductions in dose rates within remediated forest areas of 30-50% by such methods, with higher reductions achieved on open areas (Hardie & McKinley 2014, Nakayama et.al. 2015). Similar remediation factors have been observed in backpack surveys of a forest remediation trial, involving litter removal, near Iwaki (Sanderson et.al. 2016).

Another potential method for forest remediation is to cut down trees near households. This has advantages since it eliminates the risk of future deposition through litter fall and through fall (Kato et.al. 2015). However, this approach has not yet been tested, and therefore there is no data available to assess the effect of forest removal on dose rate.

Radiometric surveys using backpacks are ideal to evaluate forest dose rates and the effect of decontamination. Within forests dose is spatially highly heterogeneous, and the random distribution of tree trunks make regular grid data measurements difficult. Backpack surveys are capable of total area coverage, and can produce maps of the distribution of dose rate and radionuclide deposition. Repeat surveys can monitor the changes in the spatial distribution of dose rate due to forest decontamination work.

In the work described here, an experiment has been conducted to assess the effect of additional decontamination measures on the dose rate recorded at the edge of contaminated forests. Trees along the edge of the forest, to a distance of 10 m, have been felled, and wood chips derived from the felled trees applied to the ground surface. Assuming a density of approximately 500 kg m^{-3}, 1-2 cm of wood chips over a near-infinite surface would be expected to reduce radiocaesium full energy count rates by 10-20% and dose rates by 7-17%. When applied to smaller areas the expected reductions will be smaller. At various stages during the experiment portable gamma spectrometry methods were used to map the spatial distribution of dose rate and deposited activity within and around the remediated area. These data are used to assess the reduction in dose rate achieved at different points in the experiment.

2. Methodology

2.1 Site description

The experiment was conducted at the former Yamakiya Elementary School, Kawamata town (37°36.169N, 140°40.582E), approximately 40 km from the FDNPP. This is within the evacuated area, categorised as an area where preparations are underway to allow residents to return to their homes. The location of the site is shown in Fig. 1. The site has two connected buildings housing the elementary school and a separate building for a kindergarten, with a sports field on a levelled terrace. A forest area, with a mixture of cedar, beech, Japanese oak and red pine, is situated to the north and east of the school buildings. To the east, the forest is dominated by deciduous trees and is approximately 10 m above the school buildings with a grassed slope at approximately 45° to the kindergarten building and a small enclosed space. Beyond this, towards the south eastern part of the forest red pine are also present. To the north, the forest coniferous trees are more numerous and descends northwards below the school terrace, with the edge of the forest descending until it is level with the elementary school building. The lower parts of this slope are dominated by red pine. The forest site is being used for ongoing studies of the behaviour of radiocaesium in forest environments, including studies of interception and transfer from the forest canopy (Kato & Onda 2014, Kato et.al. 2015) and depth distribution in soils (Takahashi et.al. 2015).

Decontamination work was carried out at the school in 2012, following current practice for remediation of contaminated areas. Top soil was removed from the sports field and grassed areas around the school and replaced with sand or fresh turf between May and September 2012, and leaf litter removed from the forest areas around the school to a distance of 20 m from the forest edge between October and December 2012.

To facilitate comparisons between surveys, the site was divided into a series of areas (shown in Fig. 2); A to D for artificial surfaces around the school, Area C also includes a small ornamental garden area outside the main entrance. E to H for the forest and grassed areas. Area E was the section of forest that was felled during this work, and with area G had previously been remediated by the removal of leaf litter. Areas E, F, and G have been divided into three sub areas, and area H two sub areas. These areas are described in Table 1. Static dose rate measurements were also collected at marked positions on two overlapping grids (Fig. 2). Both grids had 10 m spacing, with one axis parallel to the edge of the forest to the east of the school. On the northern part of the site, the forest edge runs north-south, with the axes aligned along the western edge of area E2 and the southern edge of area E3. South of the kindergarten building the forest edge turns slightly to the west, resulting in a rotational offset between the grids, with the axis here aligned along the western edge of area E1.

2.2 Experimental timescale

Surveys were conducted prior to the start of the experiment, at intervals during the experiment, and following completion of the experiment. Each survey included the area of forest which was felled, and surrounding areas of forest and school grounds, but some of the surveys did not include all of the sports field and areas around the school more distant from the experimental area. Details of these measurements are given in Table 2. The trees to a distance of approximately 10 m into the forest were felled on the 8th, 9th (Areas E1 and part of E2), 12th and 13th (part of Area E2 and Area E3) November 2014, with the trunks cut and temporarily stacked on site at the edge of the remaining forest (see Fig. 3 (d)). The majority of the tree trunks were subsequently chipped on site, with the chips applied to part of the slope between the 23rd and 30th November (Area F1). Branches and other litter left on the felled area (Area E) were mostly removed between the 15th and 23rd November, with substantial stacks of branches remaining along the bottom of the slope to the east of the school buildings (the southern end of Area F1) and Area D. Following an interruption in work during the winter, the remaining area of slope (Area F2) was covered in wood chips, and the majority of the remaining piles of branches removed on the 28th April 2015 with the last few remaining material removed after that. Figure 3 shows photographs of the site at different stages of the decontamination experiment.

2.3 Instrumentation and data processing

Measurements were conducted using a Portable Gamma Spectrometry System developed at the Scottish Universities Environmental Research Centre (SUERC). The system comprises a weather proof container housing a 3x3" NaI(Tl) detector with a digital spectrometer and integrated HV supply, and a GPS receiver (Cresswell et.al. 2013). For this work, this was carried in a backpack with a measurement time of 5 s for each spectrum, corresponding to averaging the signal over a distance of approximately 2 m. As far as possible within the constraints of the terrain, a dense survey pattern of parallel lines 1-2 m apart was maintained. A netbook or tablet computer was used to power the system, and run custom software that continuously logged spectra with associated positional information, and run real-time analysis using predetermined calibration parameters. Real-time data analysis used a spectral windows with stripping algorithm to calculate activity per unit area for ^{137}Cs and ^{134}Cs, and activity per unit mass for ^{40}K, ^{214}Bi (^{238}U decay series) and ^{208}Tl (^{232}Th decay series), and a scaled count rate above 450 keV to calculate total terrestrial gamma dose rate. Analysis includes subtraction of a background recorded from a plastic boat over open water, accounting for internal activity within the detector and the cosmic dose rate. For the detector used here, these measurements were conducted on Loch Lomond, Scotland (56°8N, 4°38W), it is recognised that the sea level cosmic background is slightly higher for these measurements than would be the case in Fukushima, but this is an insignificant error compared to the terrestrial radiation. This method, applied to airborne measurements, has been described in numerous places including IAEA (1991, 2003) and Sanderson *et.al.* (1994), Cresswell *et.al.* (2006) also includes the derivation of uncertainties on measurements.

The calibration parameters for the real-time analysis, which take account of the shielding effect of the operator (Buchanan et.al. 2016), were validated using reference sites in Scotland and Japan (Cresswell et.al. 2013, Sanderson et.al. 2013). The parameters for radiocaesium and natural activity concentrations assume an open field geometry, and do not account for shielding effects from trees or contributions to the radiation measured from activity in the canopy. Measurements in a cedar forest near Iwaki demonstrated that the contribution to the measured signal from activity in the canopy is no more than a few percent, even if the canopy retains a significant fraction of the activity (Sanderson et.al. 2016). An assessment of the shielding effects of trees and understory plants is ongoing, but initial analysis suggests that this results in a reduction in count rate of less than 20% compared to the open field for forests of similar density to this site. The relative changes in activity concentration and dose rate in areas that are not physically changed during this experiment will not be affected by this attenuation effect. However, it may be necessary to consider this effect in comparing surveys of areas where trees were removed.

In open field conditions, the detector field of view is approximately 10-15 m radius, depending on source depth profile (Tyler et.al. 1996). The effect of attenuation by trees will be to reduce this field of view, to less than 10 m. This has not, however, been determined precisely to date.

For natural series radionuclides, the calibration assumes a uniform depth distribution. For radiocaesium, the calibration assumes an exponential depth distribution with a relaxation mass depth of 1.0 g cm^{-2}, which matches calibration sites established in Fukushima in 2012 (Sanderson et.al. 2013). Soil samples collected from the forest at Yamakiya between July 2011 and December 2012 (Takahashi et.al. 2015) show relaxation mass depths, excluding the litter layer, of between 0.4-0.9 g cm^{-2}. Including the litter layer and subsequent measurements (see Table S.1, Supplementary Material) the range of mass depths is 0.3-0.4 g cm^{-2}. Three soil cores collected in May 2016 at a different location within the school forest had mass depths between 0.5 and 1.1 g cm^{-2}.Therefore, although it is likely that the mass depth across the site may be less than the assumed mass depth of 1.0 g cm^{-2}, this is still appropriate for this location. The uncertainty on mass depth results in a systematic error on the activity per unit area of less than 20%, but has no impact on the relative values measured at different times assuming no change in depth profile between measurements. Measurements at a reference site on the Fukushima University just prior to field work at Yamakiya in November 2014, and at the Fukushima Prefecture Fruit Tree Research Institute in April 2015, confirmed the functionality of the detector and the validity of the calibration coefficients. These sites have been extensively sampled with activity per unit area and depth profiles determined by laboratory gamma spectrometry relative to international reference materials (Sanderson et.al. 2013).

The dose rate (μGy h^{-1}) and ^{137}Cs and ^{134}Cs activity per unit area (kBq m^{-2}) and natural series activity per unit mass (Bq kg^{-1}) have been mapped using a modified inverse distance weighting algorithm, with the average value for each map pixel being given by:

$$\bar{A} = \frac{\sum_i w_i A_i}{\sum_i w_i}$$

where the summation is across all points i within a maximum range r_{max} of the map pixel. The weight assigned to each point, w_i, is given by:

$$w_i = (r_i + \Gamma)^{-p}$$

Where r_i is the distance between the measurement point and the map pixel, Γ is a constant that flattens the distribution at small values of r_i, and p is a power. For this work, a power p=1.7, Γ=1 m and maximum range r_{max}=10 m have been used. The combination of power and flattening constant results in 95% of the weight being carried by measurements within 4 m of the pixel, approximately comparable to the field of view of the detector. The maximum range allows two-three measurements in any direction to be included in the weighted mean value.

To allow comparisons between data collected on different occasions, a spatial regridding algorithm is employed (Sanderson et.al 2004, 2008). This uses the modified inverse distance weighting algorithm to determine values for dose rate, activity per unit area or activity per unit mass in each of a grid of cells. For this work, this has been done using cells of 5x5 m, and the same parameters for the interpolation as were used to generate the mapped data.

The surveys were conducted over an extended period in autumn and spring. There is the potential for changing environmental conditions, in particular soil water content, to influence the radiometric data. If it is assumed that the activity per unit dry mass for natural radionuclides is constant then variations in the measured activity per unit mass would reflect changing soil water content. With the backpack system used here the ^{40}K peak count rate is used, the peaks used for U-series (1764 keV ^{214}Bi) and Th-series (2614 keV ^{208}Tl) activity measurement have lower intensities and are measured with lower efficiency, and hence carry substantial statistical imprecision. Ratios for different parts of the survey area are produced between the ^{40}K count rates for each survey to the first survey, with average ratios produced for the areas with predominantly artificial surfaces and the forests. A relative soil density compared to the initial survey conditions, from which a relative mean mass depth for radiocaesium can be determined. Interpolation of fluence rates for ^{137}Cs (662 keV) and ^{134}Cs (795 keV) and dose rate conversion coefficients tabulated by ICRU (1994) as a function of mass depth can then be used to adjust the measured activity per unit area for radiocaesium and dose rates to values for the environmental conditions of the initial survey.

To better understand the origins of the dose rates observed, dose rate apportionment has been used to determine the contribution of the dose rate from natural radionuclides and radiocaesium. This uses conversion factors to determine air kerma dose rate from the activity concentrations measured using the portable gamma spectrometry system, and the percentage of the total dose rate from each of these sources.

Measurements of dose rate (ambient dose, $\mu Sv\ h^{-1}$) were also collected using a TCS-172B survey meter (Aloka Hitachi Medical, Japan, calibrated by Chiyoda Technology Corporation, Japan, on September 24th 2014) at a height of 1 m. During most of the surveys, the dose rates determined with the backpack from 4-8 measurements while standing at some of these positions were also recorded.

3. Results and discussion

3.1 Detector response validation

Soil layer samples were collected on four occasions between July 2011 and December 2012 from a location within the forest to the east of the school which had not been remediated

(Takahashi et.al. 2015), with three additional samples collected on an annual basis subsequently (see Table S.1, Supplementary Material) with a mean (± standard deviation on seven measurements) activity per unit area for ^{137}Cs of 341 ± 85 kBq m^{-2} and for ^{134}Cs of 100 ± 19 kBq m^{-2} (decay corrected to November 2014). The average activity per unit area measured with the backpack system within 10 m of this location on the 8th November 2014, prior to felling of trees, was 264 ± 67 and 89 ± 23 kBq m^{-2} for ^{137}Cs and ^{134}Cs respectively. Although this single point observation of non-contemporaneous measurements is not ideal, the backpack and soil samples agree within measurement uncertainties. Together with the extensive detector validation previously conducted this does indicate that the calibration assumptions are valid for this forest environment, and suggests that the effects of attenuation by the trees and radiation from the canopy are relatively small.

During the surveys with the portable gamma spectrometry system, dose rates were recorded at some of the measurement points used to conduct dose rate measurements using the dose rate meter. Table S.2 in the supplementary material gives the dose rates recorded at these locations using the SUERC spectrometer, and measurements with the dose rate meter at similar stages in the experiment. Figure 4 shows the measurements by the two instruments at common points. The slope of a linear regression through these points reflects the approximate relationship between the different dose rate units, 1 Gy ≈ 1.2 Sv, with the small non-zero intercept probably reflecting differences in assumed instrumental background. Again, these observations support the prior validation of the backpack instrument.

3.2 Environmental conditions

As noted, there is evidence of variations in environmental conditions, probably soil water content, affecting the activity concentrations and dose rates measured by the backpack system. Average values for the activity concentrations recorded for different parts of the site for each survey are given in Table S.3 in the supplementary material. Ratios of ^{40}K activity per unit mass for each survey relative to the initial survey were used to quantify these variations. It is observed that for the artificial surfaces (areas A-D) these ratios were not significantly different from unity, and hence no corrections were required for these areas. However, within the forest (areas E-H) there were some significant variation in these ratios for different surveys, but with less variation between different parts of the forest for each survey. An average value of this ratio for all the forest areas was therefore used for each survey.

On the assumption that soil water content was the only variable, and that the ^{40}K activity per unit mass was constant with depth, these ratios can be used to calculate relative soil density changes, and hence relative mass depth changes for radiocaesium. Other factors may also contribute to variability in dose rates, including atmospheric conditions and variability in cosmic ray intensity. All the surveys were conducted in dry weather. It would be expected that air humidity and cosmic ray intensity would affect both forest and artificial areas, and the absence of an appreciable effect on the artificial surfaces suggests that these are not significant contributions to the observed variations in natural activity count rates. Correction factors for the radiocaesium activity per unit area and dose rate have been calculated using tabulated photon flux data and dose rate conversion coefficients (ICRU, 1994) for the mass depths thus estimated. The ^{40}K activity ratios, relative soil density and correction factors determined are given in Table S.4 in the supplementary material, with the corrected values also given in Table S.3.

For the surveys on the 14-15th November 2014 and 28th April 2015 the average ^{40}K activity per unit mass in the forest areas (areas E-H) was smaller than for the initial survey on the 7th-8th November 2014, suggesting that the ground was wetter at these times. Conversely, for the 23rd and 30th November 2014 and especially the 27th May 2015 the measured activity concentrations were higher, suggesting the ground was drier. It is also noted that on the 15th November 2014 survey an enhancement in ^{214}Bi activity per unit mass is measured in all areas, without corresponding variations in the ^{40}K and ^{208}Tl values, which suggests a radon related effect on that day. The impact on total dose rate is very small, and this radon effect has not been corrected for. The advantage of spectrometric measurements compared to dose rate instruments, with the use of natural activity to assess environmental conditions, is evident from these analyses.

3.3 Dose rate variation with time

The average dose rate for each area around the site, following adjustments for environmental variations and the decay of ^{134}Cs, have been plotted in Fig. 5. For the artificial surfaces around the school the dose rate is approximately constant through the experimental period, with decreases of approximately 15% for area A (sports field) and approximately 25% for area B (at the far end of the school). These are the most exposed areas on the site, and as such may be prone to enhanced weathering effects, resulting in greater redistribution of activity. Areas C (in front of the main entrance) and D (nearest the forest) have slightly higher dose rates, probably attributable to the proximity to vegetated areas, which are approximately unchanged over the duration of the surveys.

The area of forest where trees were felled (E) shows a decrease in dose rate following the felling of trees, followed by a further reduction while tree branches are removed, with no significant additional dose rate reductions following the application of wood chips to the adjacent area (F). Overall, a reduction in dose rate of 15 ± 5% is observed in this area as a result of felling the trees. The area (F) between the felled forest and the school shows initial increases in dose rate with the felling of trees, especially to the northern and southern parts of the area where tree branches were stacked. This is most likely the result of the accumulation of branches, which would carry some radiocaesium contamination, in this area. Clearing the branches and application of wood chips reduces the dose rate to 9 ± 4% below the initial values. For the forest area adjacent to the felled area (G) a dose rate reduction following the felling of trees was observed, with an increase while this area was used to stack tree branches prior to production of wood chips. After clearing these branches, an overall dose rate reduction of 12 ± 4% is observed. Area H, the control area not directly affected by the experiment, shows a large reduction in dose rate in the second part of November 2014, for reasons that are unclear, but overall only a small dose rate reduction (7 ± 3%) during the course of the experiment for most of the area. A much larger reduction in dose rate is observed for the northern part of this area (H2) in May 2015, which is also unexplained.

Dose rate apportionments for different parts of the site are shown in Fig. 6, for data recorded at each stage in the experiment. Areas A, B, C and D all have similar natural series activity concentrations, with natural dose rates of 0.050-0.055 $\mu Gy\ h^{-1}$. Area A, the school sports field, has the smallest contribution from radiocaesium to the total dose rate (65%). Areas B, C and D contain some natural surfaces with small ornamental trees, with area D adjacent to the forest area, and as a consequence have slightly higher radiocaesium concentrations from these harder to remediate surfaces (contributing 75-80% of the dose rate).

At the conclusion of the experiment, the sports field (A) remains unchanged with the other areas around the school. (B, C and D) showing a small reduction in dose rate, an average of 5 ± 3% beyond that from the physical decay of ^{134}Cs, as previously noted. In all the forest areas, the dose rate from natural series activity is approximately half that from the artificial surfaces of the school grounds (0.017-0.027 $\mu Gy\ h^{-1}$), reflecting higher natural series activity concentrations in the construction materials of the school, and potentially the sand used to replace contaminated soil, compared to the local soils. Area F, the grassed slope between the forest and the school, has natural dose rates between the two extremes reflecting contributions from both environments. The variations in natural dose rates within each area between surveys are within measurement uncertainties and demonstrate that the adjustments for soil moisture content assuming constant natural series activity have removed variations from this source. The reductions in the contributions from radioacaesium follow the same pattern as previously noted for the total dose rate.

3.5 Dose rate and ^{137}Cs distribution at different stages during the experiment

Maps of dose rate and ^{137}Cs activity per unit area for the different stages of the experiment are shown in Figs. 7 and 8. The ^{134}Cs distributions match the ^{137}Cs distributions and the corresponding maps are not reproduced here. These maps include adjustments to account for the physical decay of ^{134}Cs and changing environmental conditions.

The maps prior to felling trees (Figs 7(a) and 8(a)) clearly show the effect of earlier remediation, with the school sports fields showing dose rates below 0.15 µGy h^{-1} and ^{137}Cs below 50 kBq m^{-2}, other areas around the school showing dose rates below 0.40 µGy h^{-1} and ^{137}Cs below 150 kBq m^{-2}, and the remediated areas of the forest showing dose rates below 0.70 µGy h^{-1} and ^{137}Cs below 300 kBq m^{-2}. In contrast areas of the forest that have not been remediated show dose rates greater than 0.90 µGy h^{-1} and ^{137}Cs greater than 300 kBq m^{-2}. Comparison between the forest areas which had been remediated in 2012 and adjacent unremediated forest suggests a reduction in dose rate following remediation of approximately 35-60%, consistent with earlier studies on other sites (Nakayama et.al. 2015, Sanderson et.al. 2016).

An average dose rate of 0.1 µGy h^{-1} would result in an annual dose of approximately 1mSv. Current policy in Japan is to set a target level for protective measures in the lower part of the 1-20 mSv y^{-1} range (NSC 2011). Thus the remediated sports fields are already at this target level, but the remediated forest areas are still at the higher end of the range for the policy target.

The areas which had not been remediated in 2012 show similar values for the ^{137}Cs activity per unit area, despite variation in dominant tree type, which is consistent with previous observations at the site which showed no difference in uncalibrated ^{137}Cs count rates at ground level for deciduous and coniferous trees (Kato & Onda 2014). However, in other locations in Japan significantly elevated deposition has been observed for coniferous trees compared to deciduous (Yoshihara et.al. 2013, Sanderson et.al. 2016). This suggests local variation in the importance of foliar interception, with factors including the relative contributions of wet and dry deposition and stand density contributing.

In the areas where leaf litter was removed in 2012 there are differences observed in ^{137}Cs activity per unit area. In areas dominated by deciduous trees, predominantly to the east of the school, activity per unit area in the remediated forest ranges from approximately 100-200 kBq m^{-2}. Where coniferous trees dominate, activity per unit area is higher, between 150-250 kBq m^{-2}. It is suggested that this reflects differences in interception and subsequent transport of radiocaesium. Conifers intercepted radiocaesium in the canopy, with transfer to needles which fall to the litter layer over several years. In March 2011 the deciduous trees would not have had leaves, and consequently interception of radiocaesium in the canopy would be much lower and a larger proportion would be deposited directly onto the ground surface. Therefore, when the litter layer was removed during 2012 a larger proportion of the activity was removed from the deciduous areas. Subsequent build up of litter would have included contaminated needles from the conifers with much lower concentrations of radiocaesium in the leaves of the deciduous trees.

The maps for data recorded during the experiment (Figs. 7(b)-(e) and 8(b)-(e)) show no significant redistribution of activity over the majority of the area. The ornamental area by the school entrance becomes increasingly evident over this period. A small enhancement in dose rate to the south of the kindergarten on the 14th-15th November (Figs. 7(b) and 8(b)) corresponds to an area used to stack branches removed from the trees that had been cut down.

The final survey concentrated on measurements of the areas that had previously been used as temporary stacks for branches and other tree material (predominantly in area D and F1), and the density of observations in the forest (area H1) is significantly lower than on the previous surveys. This has resulted in the stripes evident in Figs. 7(f) and 8(f), in particular for ^{137}Cs, which are an artefact of the increased survey line spacing and are not considered to represent a difference in depositional pattern. For the area to the east of the buildings where trees were felled (areas E1 and E2), the ^{137}Cs activity per unit area at the end of the experiment is very similar to the initial state. To the north of the buildings (area E3), the corresponding area where trees were felled has a slightly higher ^{137}Cs activity per unit area. The data collected on the 28th April 2015 did not show as pronounced a soil water effect, and for these data the area to the east of the buildings (E1 and E2) shows a small decrease in ^{137}Cs activity per unit area with no significant change for the area to the north (E3). It appears that the effect of tree felling in reducing the ^{137}Cs inventory is different for these two areas, with it being more effective to the east of the buildings than the north.

Figure 9 shows the change in dose rate for the areas of main interest for this study, after regridding to allow for corrections due to environmental change and the physical decay of ^{134}Cs. The uncertainties propagated through the analysis result in typically 5-10% uncertainty on this change, corresponding to one or two colour divisions, with uncertainties being larger where the measurement density is lower and near the edges of the survey areas. The combination of measurement uncertainties and local redistribution of activity, over ranges of a few meters, results in a complicated visual pattern. However, some general observations can still be made from these maps of dose rate change. There are small reductions in dose rate observed with the felling of the trees (area E) particularly evident in Fig. 9(c), accompanied by temporary increases in dose rate in locations where cut branches were stacked prior to removal (to the north and south of the kindergarten, parts of areas D and F1) in Figs. 9(a)-9(c). Removal of the litter generated during the felling, and accumulated since the 2012 decontamination, had a very small impact on dose rate with the exception of locations where this included removal of some of the stored branches, seen in comparisons of area D in Figs 9(a)-9(c) compared to 9(d). The area to which wood chips had been applied (to the south and east of the kindergarten, areas F1 and F2) shows a small further reduction in dose rate in Fig. 9(e).

4. Conclusions

The various measurements presented here all support the conclusion that, on this site, felling trees coupled with the use of wood chips to cover the ground has produced reductions of 15±5% in the dose rate for the area which was cleared, and slightly smaller dose rate reductions in adjacent areas both within the forest (12±4%) and in the open areas adjacent to the forest (9±4%). However, it also noted that 7±3% reductions are measured in some of the areas of forest which were not subject to remediation, after consideration of the decay of ^{134}Cs. Radiometric surveys on a cedar plantation near Iwaki have demonstrated reductions in dose rate of 10-15% over a year in some unremediated areas (Sanderson et.al. 2016), which is not dissimilar to the reductions observed here. If similar reductions in dose rate would have occurred in the remediated areas as a result of natural redistributive processes then this reduces the overall effectiveness of the remediation conducted in these areas to approximately 10-15% reductions in dose rate. The reductions in dose rate that might be achieved on other sites are likely to be variable, with dependencies on the particular characteristics of each site, including tree species and topography.

Although the felling of trees has a substantial impact on forest ecology, this does have an appreciable immediate impact on dose rates near the forest edge which will contribute to overall dose rate reductions in contaminated areas and ultimately to allowing evacuated residents to return to their homes. It is expected that the removal of trees, and hence a source of contaminated litterfall, will result in additional long term radiological benefits by reducing routes for recontamination of the remediated area. The Yamakiya study site will continue to be monitored over the next few years to evaluate this.

The dosimetry method using the convenient and sophisticated backpack system used in this work is widely applicable to decontamination work, and other studies, in Fukushima.

Supplementary Material

Table S.1: Data from scraper plate measurements at the Yamakiya school forest, July 2011 to 2015, and three cores collected in May 2016 from a second location within the forest.

Table S.2: Spot measurements (μGy h^{-1} with the backpack, μSv h^{-1} with the TCS-172B dose rate meter) at the marked dose rate measurement points

Table S.3: Mean values for ^{134}Cs and ^{137}Cs activity per unit area, ^{40}K, ^{214}Bi and ^{208}Tl activity per unit mass and dose rate measured with the backpack system for different areas of the Yamakiya site. Values in italics have been adjusted to correct for variable environmental conditions and with ^{134}Cs decay corrected to 8th November 2014.

Table S.4: Ratio of the mean ^{40}K count rates for each survey relative to the initial survey on the 7-8th November 2014, for the hard surface areas and the forest areas. For the forest area the relative soil density is given, and correction factors for both radiocaesium and dose rate calculated from this relative soil density difference.

Acknowledgments

We thank Kawamata Town Office for permission to access the Yamakiya Elementary School grounds and the surrounding forest for this study. Our thanks are also due to Mr Sato and Ms Chiba for assistance clearing branches and spreading wood chips.
This research was financially supported by KAKENHI Grant Number 24110001 and 24110006, and part of the distribution-mapping project, which was financed by the Ministry of Education, Culture, Sports, Science, and Technology, and the project on integrating distribution data and development of transfer model regarding radioactive substances derived from Fukushima Daiichi Nuclear Power Plant accident financed by the Nuclear Regulation Authority, Japan. Funding was also provided through the forest project of the Institute of Environmental Radioactivity, Fukushima University.

References

Buchanan, E.; Cresswell, A.J.; Seitz, B.; Sanderson, D.C.W. Operator related attenuation effects in radiometric surveys. *Radiation Measurements* **2016**, *86*, 24-31; doi 10.1016/j.radmeas.2015.15.029.

Cresswell, A.J.; Sanderson, D.C.W.; Harrold, M.; Kirley, B.; Mitchell, C.; Weir, A. Demonstration of lightweight gamma spectrometry systems in urban environments. *Journal of Environmental Radioactivity* **2013**, *124*, 22-28; DOI 10.1016/j.jenvrad.2013.03.006

Cresswell, A.J.; Sanderson, D.C.W.; White, D.C. 137Cs measurement uncertainties and detection limits for airborne gamma spectrometry (AGS) data analysed using a spectral windows method. *Applied Radiation and Isotopes* **2006**, *64*, 247-253; DOI 10.1016/j.apradiso.2005.07.013

Hardie, S. M. L.; McKinley, I. G. Fukushima remediation: status and overview of future plans. *Journal of Environmental Radioactivity* **2014**, *133*, 75-85; DOI 10.1016/j.jenvrad.2013.08.002

Hashimoto, S.; Matsuura, T.; Nanko, K.; Linkov, I.; Shaw, G.; Kaneko, S. Predicted spatio-temporal dynamics of radiocesium deposited onto forests following the Fukushima nuclear accident. *Scientific Reports* **2013**, *3*, srep02564. DOI: 10.1038/srep02564.

Airborne Gamma Ray Spectrometer Surveying; International Atomic Energy Agency: Vienna, 1991; Technical Reports Series 323.

Guidelines for Radioelement Mapping Using Gamma Ray Spectrometry Data. International Atomic Energy Agency: Vienna, 2003; IAEA-TECDOC-1363.

Gamma-ray Spectrometry in the Environment. International Commission on Radiation Units and Measurements: Bethesda, 1994. ICRU Report No. 53. ISBN 0-913394-52-1

Kato, H.; Onda, Y. Temporal changes in the transfer of accidentally released 137Cs from tree crowns to the forest floor after the Fukushima Daiichi Nuclear Power Plant accident. *Progress in Nuclear Science and Technology* **2014**, *4*, 18-22.

Kato, H., Onda, Y., Hisadome, K., Loffredo, N., Kawamori, A. Temporal changes in radiocesium deposition in various forest stands following the Fukushima Dai-ichi Nuclear Power Plant accident. *Journal of Environmental Radioactivity* **2015**. doi:10.1016/j.jenvrad.2015.04.016

Nakayama, S.; Kawase, K.; Hardie, S.; Yashio, S.; Iijima, K.; Mckinley, I.; Miyahara, K.; Klein, L. *Remediation of Contaminated Areas in the Aftermath of the Accident at the Fukushima Daiichi Nuclear Power Station: Overview, Analysis and Lessons Learned. Part 1: A Report on the "Decontamination Pilot Project"* Japan Atomic Energy Agency, 2015; JAEA-Review 2014-051. doi: 10.11484/jaea-review-2014-051

Basic Policy of the Nuclear Safety Commission of Japan on Radiation Protection for Termination of Evacuation and Reconstruction. Nuclear Safety Commission of Japan, 2011; 54th Nuclear Safety Commission Reference No. 4. http://www.nsr.go.jp/archive/nsc/NSCenglish/geje/20110719suggest_4.pdf

Sanderson, D.C.W.; Cresswell, A.J.; Tamura, K.; Iwasaka, T.; Matsuzaki, K. Evaluating remediation of radionuclide contaminated forest near Iwaki, Japan, using radiometric methods. *Journal of Environmental Radioactivity* **2016**, *162-163*, 118-128. doi: 10.1016/j.jenvrad.2016.05.019

Sanderson, D.C.W.; Cresswell, A.J.; Seitz, B.; Yamaguchi, K.; Takase, T.; Kawatsu, K.; Suzuki, C.; Sasaki, M. *Validated Radiometric Mapping in 2012 of Areas in Japan Affected by the Fukushima-Daiichi Nuclear Accident*. University of Glasgow:Glasgow, UK, 2013; ISBN 978-0-85261-937-7; http://eprints.gla.ac.uk/86365/

Sanderson, D.C.W.; Cresswell, A.J.; White D.C. The effect of flight line spacing on radioactivity inventory and spatial feature characteristics of airborne gamma-ray spectrometry data. *International Journal of Remote Sensing* **2008**, *29*, 31–46; DOI 10.1080/01431160701268970

Sanderson, D.C.W.; Cresswell, A.J.; Scott, E.M.; Lang, J.J. Demonstrating the European capability for airborne gamma spectrometry: results from the ECCOMAGS exercise. *Radiation Protection Dosimetry* **2004**, *109*, 119-125; DOI 10.1093/rpd/nch243

Sanderson, D. C. W.; Allyson, J. D.; Tyler A. N. Rapid quantification and mapping of radiometric data for anthropogenic and technically enhanced natural nuclides. In *Application of Uranium Exploration Data and Techniques in Environmental Studies*; IAEA: Vienna 1994; IAEA TECDOC-827. pp 197-216.

Takahashi, J.; Tamura, K.; Suda, T.; Matsumura, R.; Onda, Y. Vertical distribution and temporal changes of 137Cs in soil profiles under various land uses after the Fukushima Dai-ichi Nuclear Power Plant accident. *Journal of Environmental Radioactivity* **2015**, *139*, 351-361; DOI 10.1016/j.jenvrad.2014.07.004

Tyler, A.N., Sanderson, D.C.W., Scott, E.M., Allyson, J.D. Accounting for Spatial Variability and Fields of View in Environmental Gamma Ray Spectrometry. *Journal of Environmental Radioactivity* **1996**, *33*, 213-235.

Yoshihara, T.; Matsumura, H.; Hashida, S.; Nagaoka, T. Radiocesium contaminations of 20 wood species and the corresponding gamma-ray dose rates around the canopies at 5 months after the Fukushima nuclear power plant accident. *Journal of Environmental Radioactivity* **2013**, *115*, 60-68. doi: 10.1016/j.jenvrad.2012.07.002

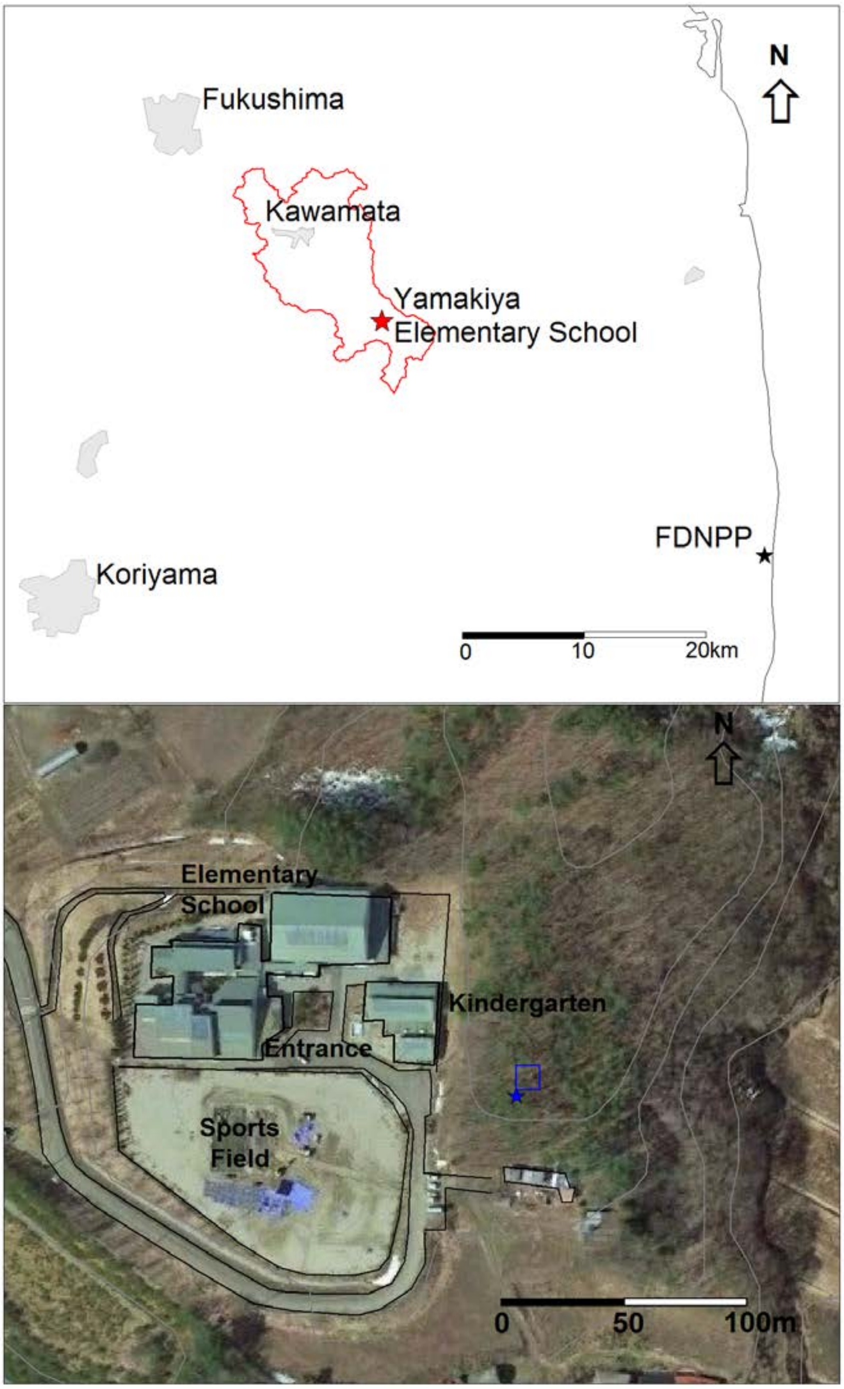

Figure 1. Location of the former Yamakiya Elementary School and forest (top), and the buildings within the school (bottom). The location of the Takahashi et.al. (2015) sampling site is indicated by the blue star, just to the south of the monitoring tower (Kato and Onda 2014, Kato et.al. 2015) indicated by the blue square. Aerial photograph © 2015 Google. Image © 2015 ZENRIN.

Figure 2. Location of survey area divisions (top), and dose rate measurement grids (bottom).

Aerial photograph © 2015 Google. Image © 2015 ZENRIN.

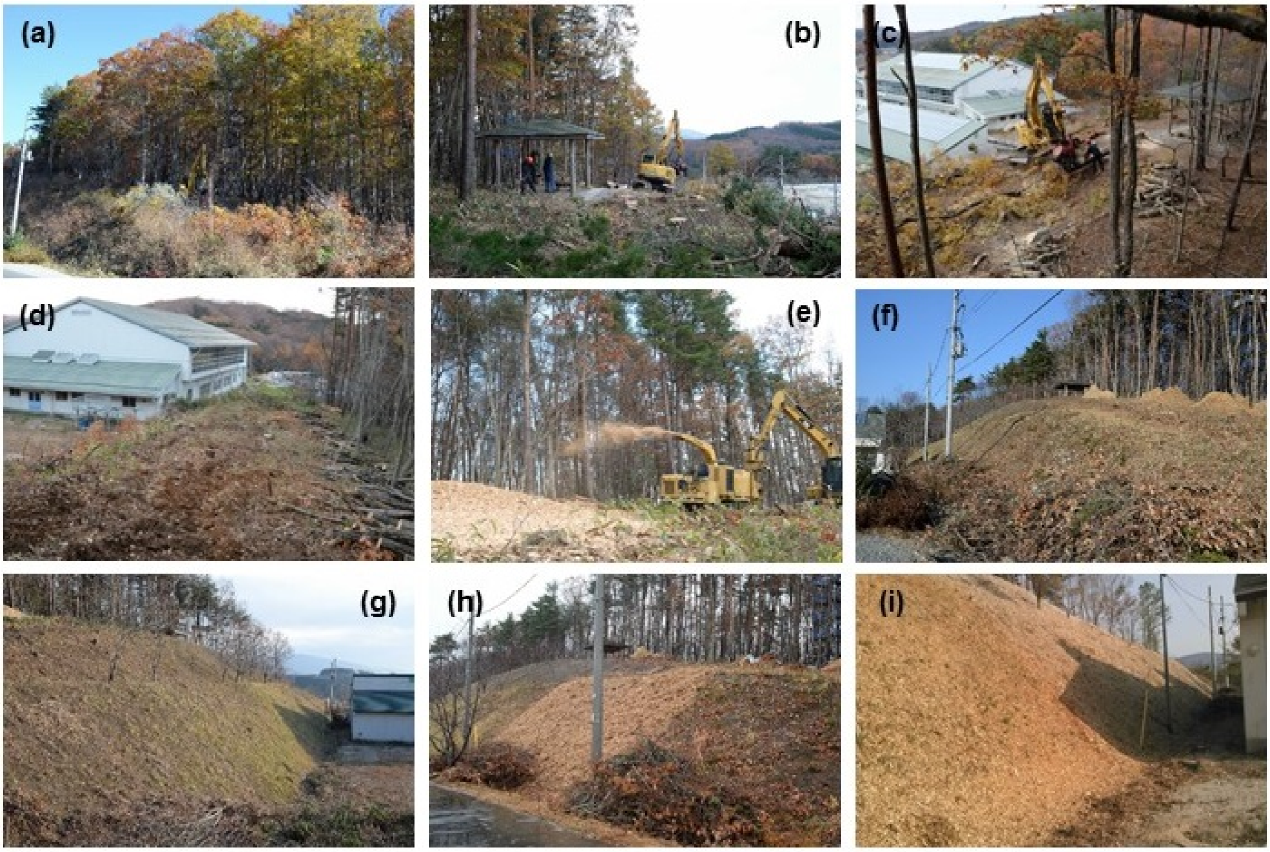

Figure 3. Photographs illustrating the different stages of remediation. (a) area E1 before felling of trees, (b)-(c) areas E1 and E2 during tree felling, (d) area E1 after felling of trees, (e) production of wood chips in area E2, (f) area F1 and (g) area F2 after production of wood chips, (h) after application of wood chips on part of area F1, and (i) after application of wood chips to whole of areas F1 and F2.

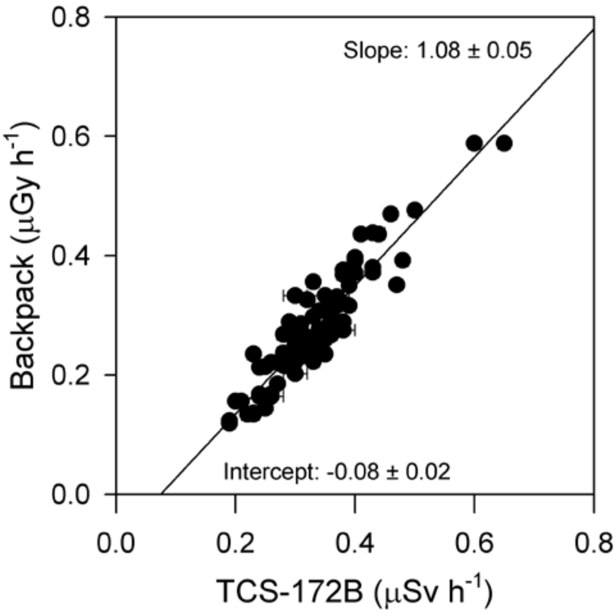

Figure 4. Comparison between dose rates measured with a survey meter and the backpack system.

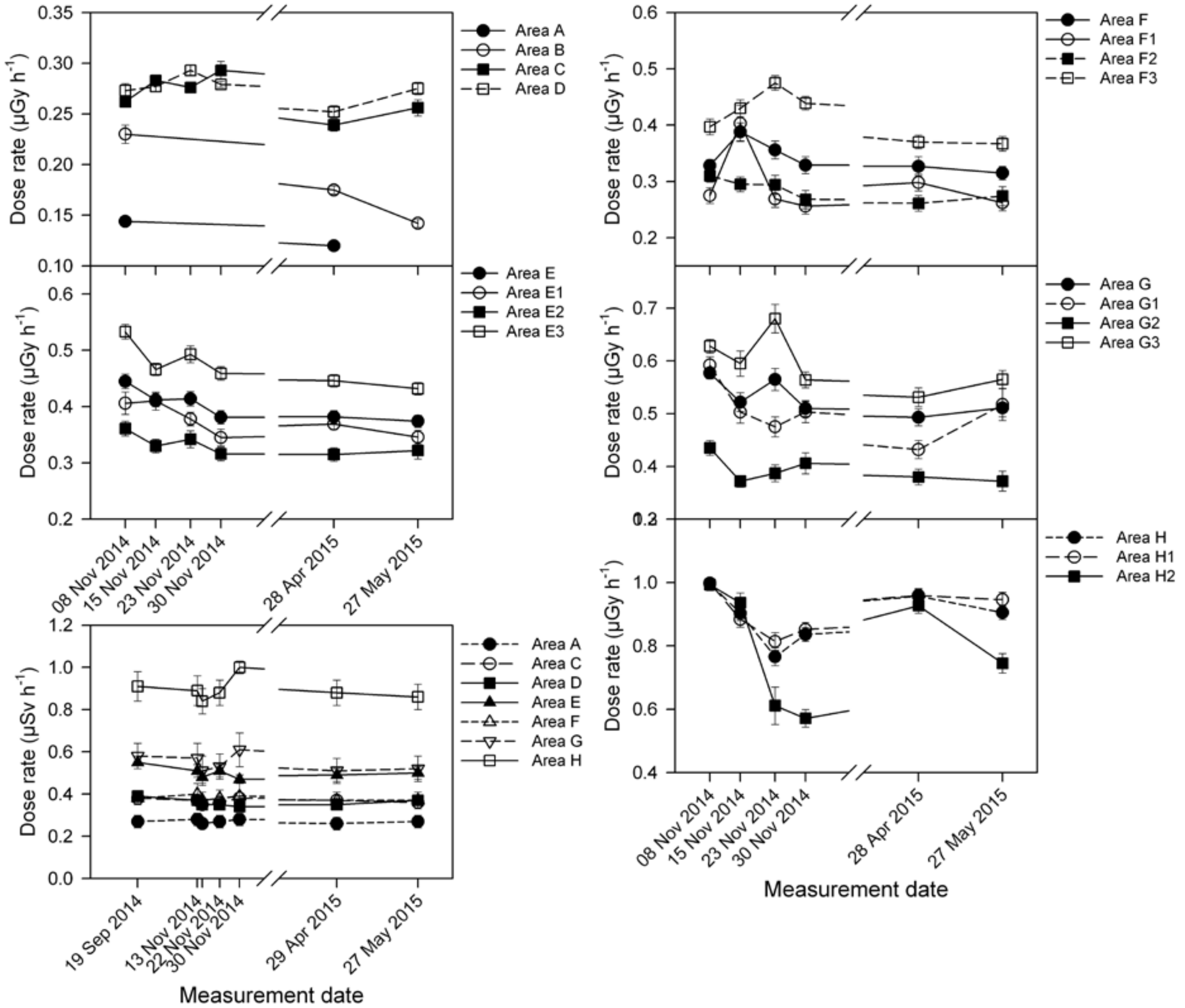

Figure 5. Variation in dose rate measured with the backpack system, after adjustments for environmental variations and ^{134}Cs decay, with time for the artificial surfaces (A-D, top left), the forest area that had been felled (E, middle left), the slope between the felled forest and the school (F, top right), the unfelled forest previously remediated (G, middle right) and the rest of the forest (H, bottom). Dose rate measurements with the TCS-172B survey meter are shown (bottom left)

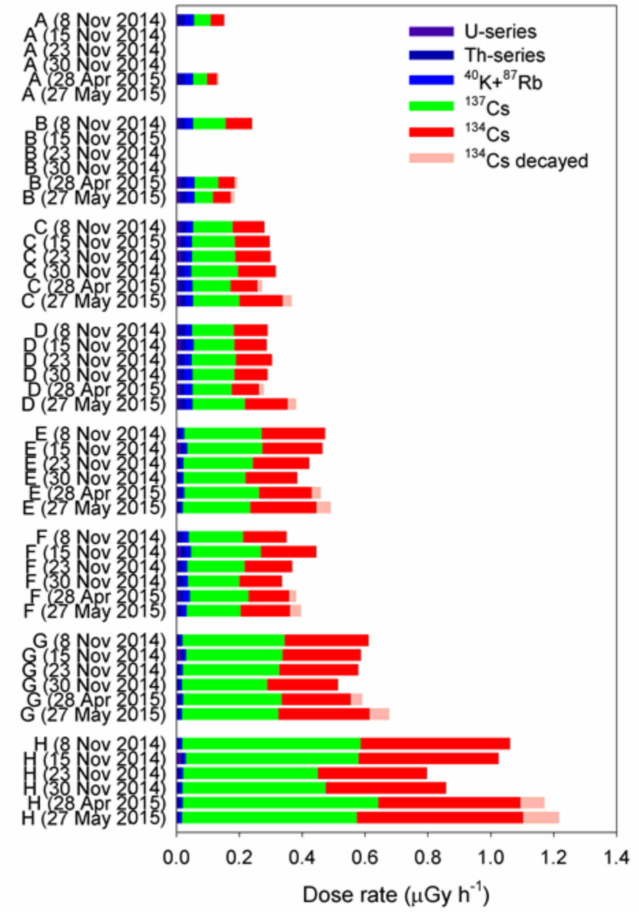

Figure 6. Dose rate apportionments at different parts of the site, as shown in Fig. 2 and listed in Table 1, at each stage of the experiment. The areas that have been sub-divided in Fig. 2 have been combined here.

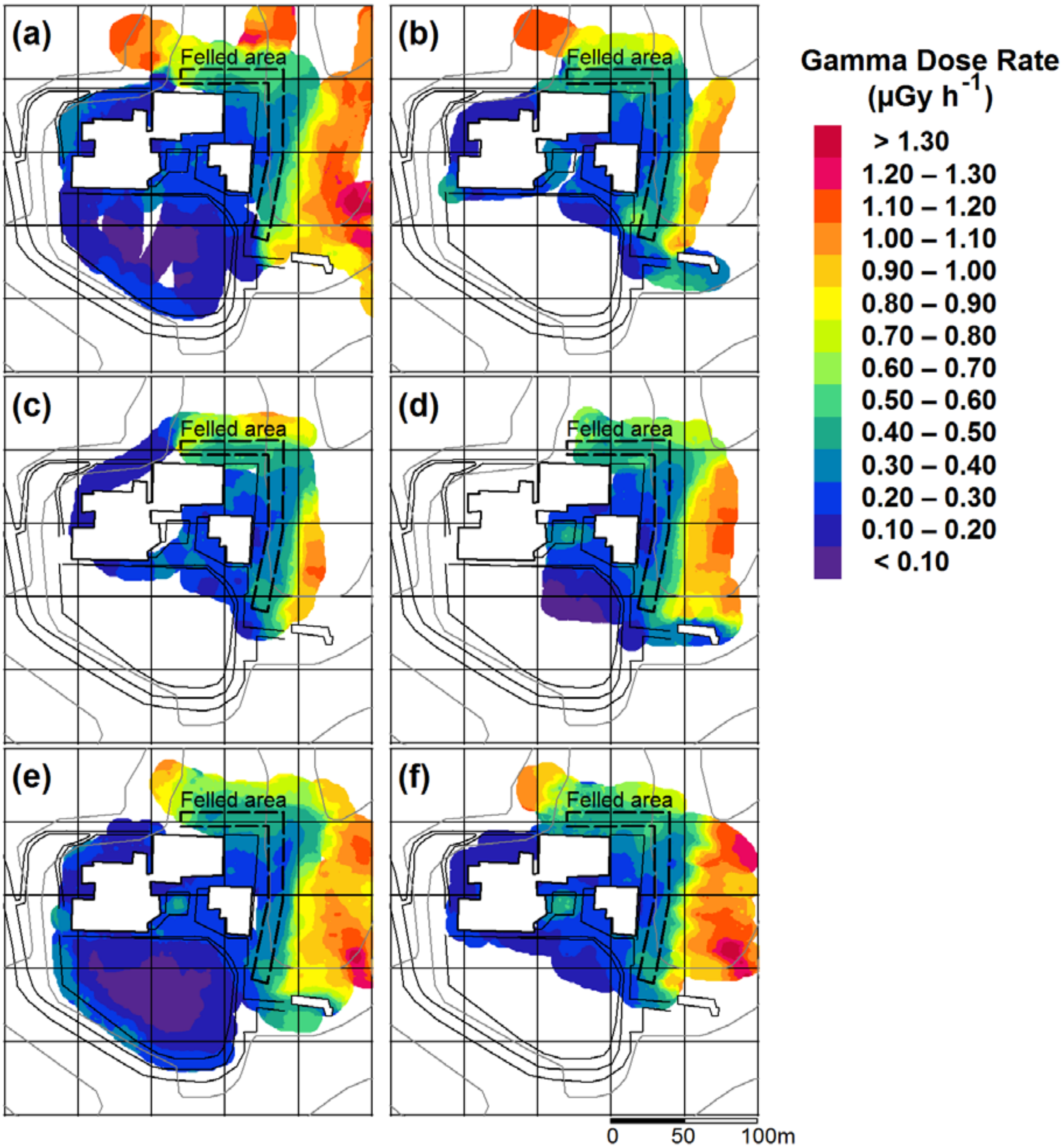

583 **Figure 7.** Gamma dose rate distribution during the experiment. (a) 7th-8th November 2014,
584 (b) 14th-15th November 2014, (c) 23rd November 2014, (d) 30th November 2014, (e) 28th April
585 2015 and (f) 27th May 2015.

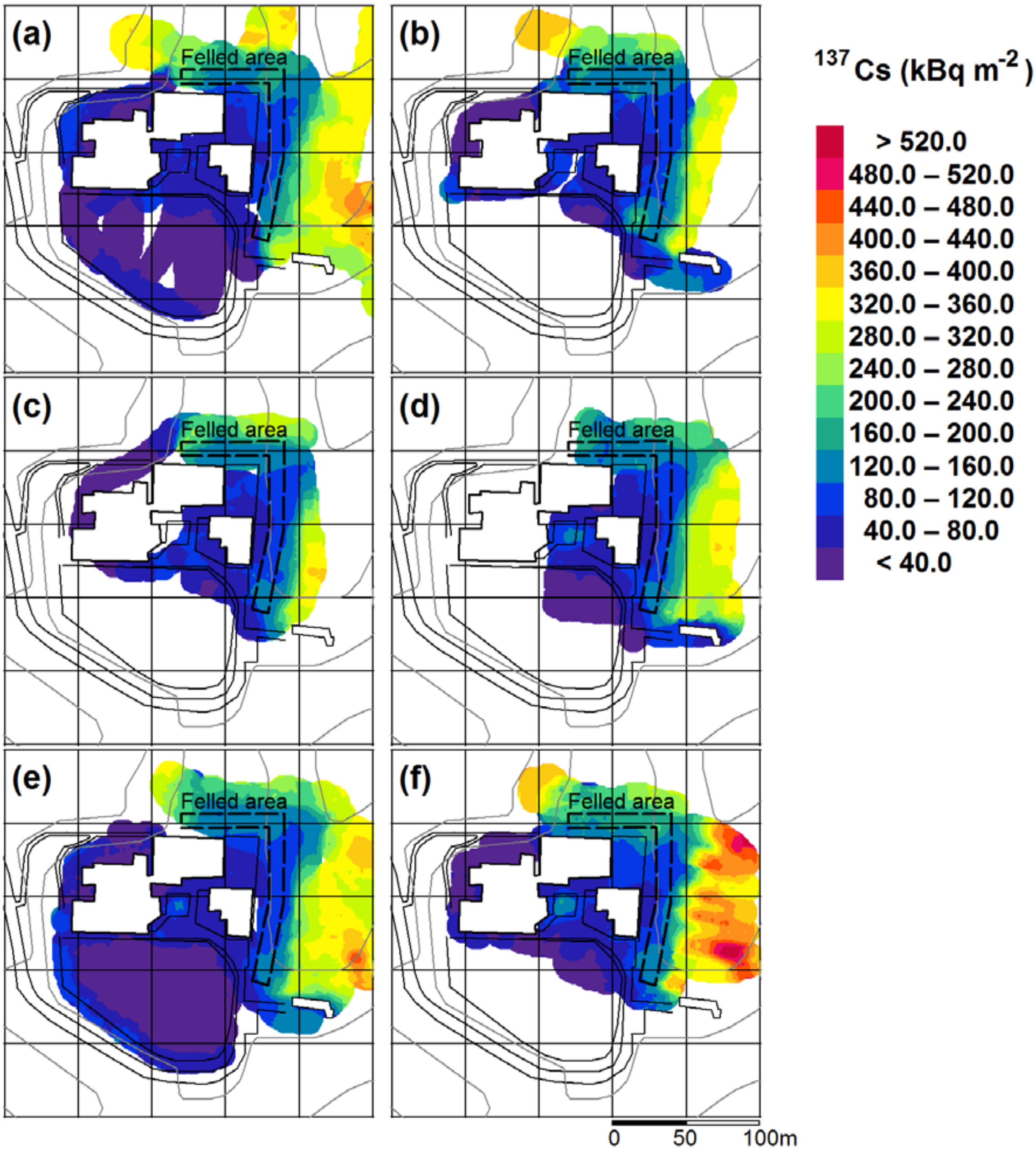

Figure 8. ^{137}Cs activity per unit area distribution during the experiment. (a) 7th-8th November 2014, (b) 14th-15th November 2014, (c) 23rd November 2014, (d) 30th November 2014, (e) 28th April 2015 and (f) 27th May 2015.

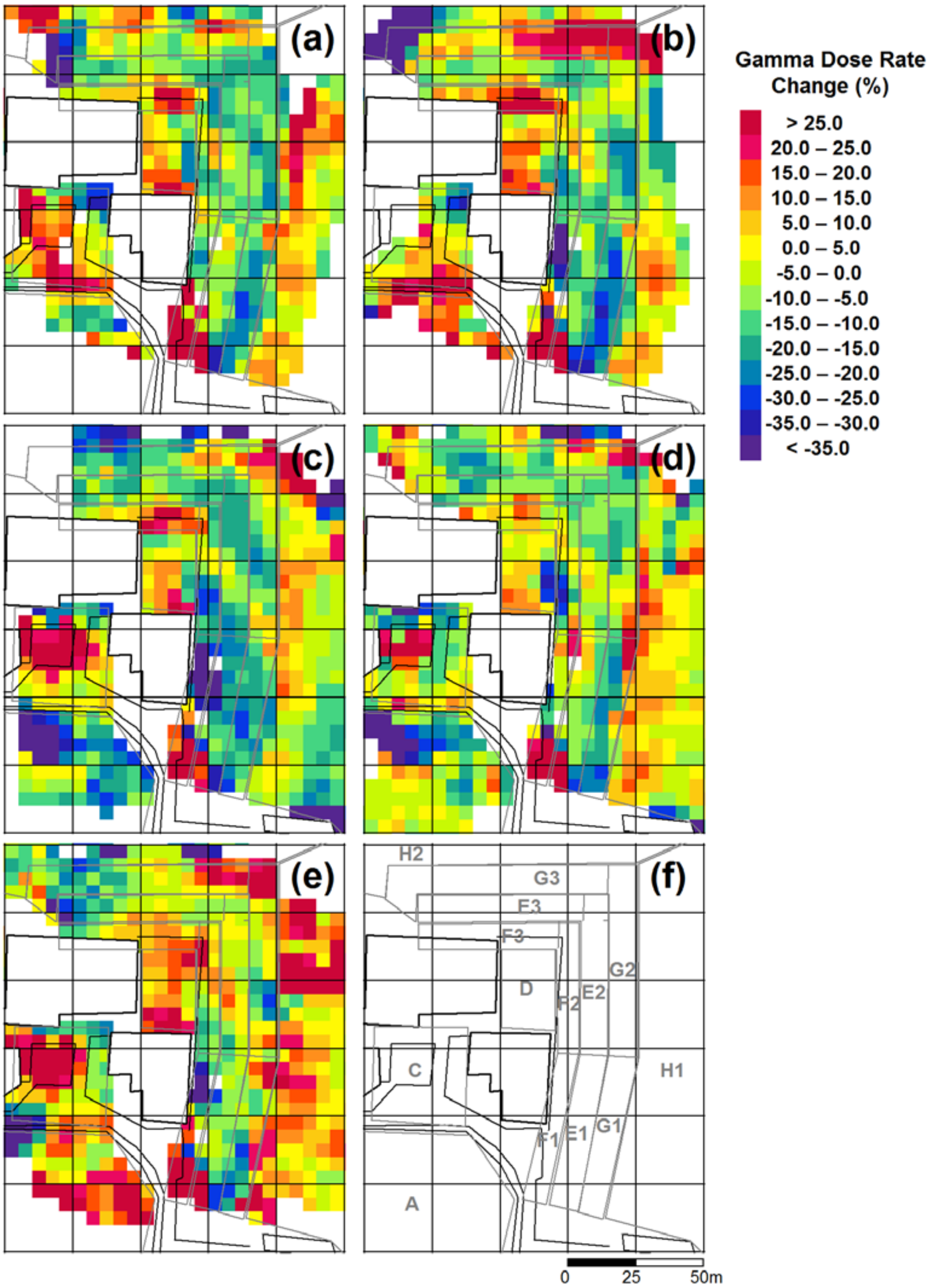

Figure 9. Dose rate changes relative to the initial survey (7-8th November 2014), with oranges and reds indicating an increase in dose rate and greens and blues a decrease, following corrections for environmental conditions and physical decay. Uncertainties are typically 5-10% (one or two colour bands) (a) Following removal of trees (14-15th November 2014), (b) following removal of litter (23rd November 2014), (c) following application of wood chips to part of the site (30th November 2014), (d) following completion of application

of wood chips (28th April 2015) and (e) following removal of the last of the cut trees (27th May 2015). The subdivided areas (Fig.2 and Table 1) are indicated by the grey lines, and labelled (f).

Area	Description
A	Sports field south of the school buildings
B	Footpath and line of trees to the north and west of the two parts of the Elementary School building
C	Area outside the Elementary School entrance, between the school and kindergarten, including an ornamental shrubbery
D	Open area to the north of the kindergarten and east of the Elementary school buildings
E	10 m wide forested area along the top of the slope east of the school buildings and to the north of area D. This is subdivided into three sub-areas; E1 and E2 to the east of the school buildings, E3 to the north. This area had previously been remediated by removal of leaf litter. Trees in this area were felled for this experiment.
F	Slope between the forest and the school buildings, which levels off at the western end of the northern section. This is subdivided into three sub-areas; F1 and F2 to the east of the school buildings, F3 to the north. Wood chips were applied to sub-areas E1 and E2 for this experiment.
G	10 m wide strip of forest to the east and north of area E. This is subdivided into three sub-areas; G1 and G2 to the east of the school buildings, G3 to the north. This area had previously been remediated with the removal of leaf litter.
H	The remaining forestry around the school. This is subdivided into two sub-areas; H1 to the east and H2 to the north. Sub-area H1 is mixed woodland, sub-area H2 includes stands of red pine.

Table 1: Description of survey area divisions shown in Fig. 2.

Date	Stage	Area surveyed	Approximate number of measurements
7^{th}-8^{th} Nov 2014	Prior to tree felling	School grounds, all forest to the east, parts of forest to the north including all areas previously remediated	1500
14^{th}-15^{th} Nov 2014	After tree felling	School grounds excluding playground, forest 10-20 m beyond felled area	1200
23^{rd} Nov 2014	Following removal of litter	School grounds excluding playground, forest 10-20 m beyond felled area	700
30^{th} Nov 2014	Following application of wood chips to part of the area	School grounds within 50 m of forest, forest 10-20 m beyond felled area	700
28^{th} Apr 2015	Following removal of cut wood around school and application of wood chips to entire area	School grounds, all forest to the east, parts of forest to the north including all areas previously remediated	1800
27^{th} May 2015	Following removal off all branches and other material	School grounds within 50 m of forest, all forest areas	1000

Table 2. Summary of surveys conducted.